Propofol (Diprivan®) and Intralipid® Exacerbate Insulin Resistance in Type-2 Diabetic Hearts by Impairing GLUT4 Trafficking

Lou, Phing-How ; Lucchinetti, Eliana ; Zhang, Liyan ; Affolter, Andreas ; Gandhi, Manoj ; Zhakupova, Assem ; Hersberger, Martin ; Hornemann, Thorsten ; Clanachan, Alexander S ; Zaugg, Michael

Abstract: BACKGROUND The IV anesthetic, propofol, when administered as fat emulsion-based formulation (Diprivan) promotes insulin resistance, but the direct effects of propofol and its solvent, Intralipid, on cardiac insulin resistance are unknown. METHODS Hearts of healthy and type-2 diabetic rats (generated by fructose feeding) were aerobically perfused for 60 minutes with 10 M propofol in the formulation of Diprivan or an equivalent concentration of its solvent Intralipid (25 M) ± insulin (100 mU • L). Glucose uptake, glycolysis, and glycogen metabolism were measured using [H]glucose. Activation of Akt, GSK3 , AMPK, ERK1/2, p38MAPK, S6K1, JNK, protein kinase C (PKC), and protein kinase CC II (PKC II) was determined using immunoblotting. GLUT4 trafficking and phosphorylations of insulin receptor substrate-1 (IRS-1) at Ser307(h312), Ser1100(h1101), and Tyr608(hTyr612) were measured. Mass spectrometry was used to determine acylcarnitines, phospholipids, and sphingolipids. RESULTS Diprivan and Intralipid reduced insulin-induced glucose uptake and redirected glucose to glycogen stores in diabetic hearts. Reduced glucose uptake was accompanied by lower GLUT4 trafficking to the sarcolemma. Diprivan and Intralipid inactivated GSK3 but activated AMPK and ERK1/2 in diabetic hearts. Only Diprivan increased phosphorylation of Akt(Ser473/Thr308) and translocated PKC and PKC II to the sarcolemma in healthy hearts, whereas it activated S6K1 and p38MAPK and translocated PKC II in diabetic hearts. Furthermore, only Diprivan phosphorylated IRS-1 at Ser1100(h1101) in healthy and diabetic hearts. JNK expression, phosphorylation of Ser307(h312) of IRS-1, and PKC expression and translocation were increased, whereas GLUT4 expression was reduced in insulin-treated diabetic hearts. Phosphatidylglycerol, phosphatidylethanolamine, and C18-sphingolipids accumulated in Diprivan-perfused and Intralipid-perfused diabetic hearts. CONCLUSIONS Propofol and Intralipid promote insulin resistance predominantly in type-2 diabetic hearts.

DOI: https://doi.org/10.1213/ANE.0000000000000558

Propofol (Diprivan®) and Intralipid® Exacerbate Insulin Resistance in Type-2 Diabetic Hearts by Impairing GLUT4 Trafficking

Phing-How Lou, PhD,* Eliana Lucchinetti, PhD,† Liyan Zhang, PhD,† Andreas Affolter, BSc,‡ Manoj Gandhi, PhD,§ Assem Zhakupova, MS,‖ Martin Hersberger, PhD,‡ Thorsten Hornemann, PhD,‖ Alexander S. Clanachan, PhD,§ and Michael Zaugg, MD, MBA, FRCPC†

BACKGROUND: The IV anesthetic, propofol, when administered as fat emulsion-based formulation (Diprivan®) promotes insulin resistance, but the direct effects of propofol and its solvent, Intralipid® , on cardiac insulin resistance are unknown.

METHODS: Hearts of healthy and type-2 diabetic rats (generated by fructose feeding) were aerobically perfused for 60 minutes with 10 μM propofol in the formulation of Diprivan or an equivalent concentration of its solvent Intralipid (25 μM) ± insulin (100 mU · L^{-1}). Glucose uptake, glycolysis, and glycogen metabolism were measured using [^{3}H]glucose. Activation of Akt, GSK3β, AMPK, ERK1/2, p38MAPK, S6K1, JNK, protein kinase Cθ (PKCθ), and protein kinase CCβ_{II} (PKCβ_{II}) was determined using immunoblotting. GLUT4 trafficking and phosphorylations of insulin receptor substrate-1 (IRS-1) at Ser307(h312), Ser1100(h1101), and Tyr608(hTyr612) were measured. Mass spectrometry was used to determine acylcarnitines, phospholipids, and sphingolipids.

RESULTS: Diprivan and Intralipid reduced insulin-induced glucose uptake and redirected glucose to glycogen stores in diabetic hearts. Reduced glucose uptake was accompanied by lower GLUT4 trafficking to the sarcolemma. Diprivan and Intralipid inactivated GSK3β but activated AMPK and ERK1/2 in diabetic hearts. Only Diprivan increased phosphorylation of Akt(Ser473/Thr308) and translocated PKCθ and PKCβ_{II} to the sarcolemma in healthy hearts, whereas it activated S6K1 and p38MAPK and translocated PKCβ_{II} in diabetic hearts. Furthermore, only Diprivan phosphorylated IRS-1 at Ser1100(h1101) in healthy and diabetic hearts. JNK expression, phosphorylation of Ser307(h312) of IRS-1, and PKCθ expression and translocation were increased, whereas GLUT4 expression was reduced in insulin-treated diabetic hearts. Phosphatidylglycerol, phosphatidylethanolamine, and C18-sphingolipids accumulated in Diprivan-perfused and Intralipid-perfused diabetic hearts.

CONCLUSIONS: Propofol and Intralipid promote insulin resistance predominantly in type-2 diabetic hearts. (Anesth Analg 2015;120:329–40)

Insulin resistance first develops in the heart[1] well before its onset in other peripheral organs including the skeletal muscle. Cardiac insulin resistance is defined as the reduced ability of myocytes to increase glucose uptake in response to insulin stimulation.[2] It is of importance because it reduces tolerance against ischemia–reperfusion injury and increases infarct size due to the loss of metabolic flexibility and endothelial dysfunction.[3] Insulin resistance is accompanied by significant morbidity and mortality, independent of other established risk factors. Even in the absence of hyperglycemia or overt diabetes, insulin resistance is closely associated with coronary artery disease,[4] congestive heart failure,[5] atherosclerosis, and cerebral stroke.[6]

Diprivan® (AstraZeneca Inc., Mississauga, ON, Canada), a fat emulsion-based propofol formulation, was recently shown to promote insulin resistance.[7] It increased insulin levels but did not change blood glucose concentrations, resulting in a markedly reduced quantitative insulin sensitivity check index, an index of insulin sensitivity.[7] However, from that observation, it is unclear whether propofol or its solvent Intralipid® is causally involved in the generation of insulin resistance. In clinical practice, fat emulsions are commonly used as solvents to administer lipophilic drugs such as propofol or to provide IV nutrition to patients.[8] Even short IV infusions of fat emulsions were previously reported to impair insulin sensitivity (which determines whole body glucose disposal) in healthy nondiabetic volunteers,[9] but the effects of Intralipid on cardiac insulin resistance are unknown. In this study, we sought to determine whether propofol, or its solvent Intralipid, alters glucose utilization in healthy and type-2 diabetic hearts and, if so,

From the *Department of Anesthesiology and Pain Medicine and Department of Pharmacology, University of Alberta, Edmonton, Canada; †Department of Anesthesiology and Pain Medicine, University of Alberta, Edmonton, Canada; ‡Department of Clinical Chemistry, University Children's Hospital Zurich, Zurich, Switzerland; §Department of Pharmacology, University of Alberta, Edmonton, Canada; and ‖Department of Clinical Chemistry, University Hospital Zurich, Zurich, Switzerland.

Liyan Zhang, PhD, is currently affiliated with Department of Pediatrics, University of Alberta, Edmonton, Canada.

Accepted for publication September 24, 2014.

Funding: The study was supported by grants from the Heart and Stroke Foundation of Alberta, Northwest Territories, and Nunavut (Canada); the Canadian Institutes of Health Research grant MOP115055; and a grant from the Mazankowski Alberta Heart Institute, Edmonton, Canada.

The authors declare no conflicts of interest.

Drs. Lou, Lucchinetti, Clanachan, and Zaugg contributed equally to this manuscript.

Supplemental digital content is available for this article. Direct URL citations appear in the printed text and are provided in the HTML and PDF versions of this article on the journal's website (www.anesthesia-analgesia.org).

Reprints will not be available from the authors.

Address correspondence to Michael Zaugg, MD, MBA, FRCPC, Department of Anesthesiology and Pain Medicine, University of Alberta, CSB Room 8–120, Edmonton AB T6G 2G3, Canada. Address e-mail to michael.zaugg@ualberta.ca.

DOI: 10.1213/ANE.0000000000000558

how insulin signaling would be affected by these treatments. Specifically, we hypothesized that both propofol and Intralipid would increase insulin resistance in the already metabolically compromised diabetic heart. To address this aim, we compared the effects of the 2 commercially available drugs Diprivan and Intralipid. The use of the working rat heart model allowed us to conduct the experiments under well-controlled conditions, independent of multiple confounding factors resulting from alterations in whole body physiology. For our experiments, we used hearts from fructose-fed rats, a well-established model of type-2 diabetes with hyperglycemia, hyperinsulinemia, hypertriglyceridemia, insulin resistance, arterial hypertension, and abdominal obesity, consistent with all features of the human metabolic syndrome.[10,11] Moreover, fructose-induced dietary diabetes resembles early type-2 diabetes,[12] which is potentially reversible and devoid of the severe maladaptive consequences typically accompanying genetic or inbred models of diabetes mellitus.

METHODS

The investigation conforms to the Guide for the Care and Use of Laboratory Animals published by the U.S. National Institutes of Health (NIH Publication No. 85-23, revised 1996), and the experimental protocol used in this investigation was approved by the University of Alberta Animal Policy and Welfare Committee. All materials were from Sigma-Aldrich (St. Louis, MO) unless otherwise stated.

Model of Type-2 Diabetes Mellitus Using Fructose Feeding

Male Sprague-Dawley rats (8 weeks of age, from the Biosciences breeding colony, University of Alberta, Edmonton, Canada) were fed for 6 weeks with standard chow (PicoLab® Laboratory Rodent diet 5LOD, LabDiet Inc., St. Louis, MO) and fructose (10% w/v) dissolved in drinking water and compared with untreated rats fed a fructose-free diet. The lipogenic sugar fructose, as opposed to glucose, feeds directly into the pool of C2-bodies in the liver causing increased hepatic triglyceride formation, followed by hyperlipidemia and insulin resistance. After only 6 weeks of fructose feeding, rats consistently exhibit the classical characteristics of type-2 diabetes including hyperglycemia, hyperinsulinemia, hypertriglyceridemia, insulin resistance, arterial hypertension, and abdominal obesity. This type-2 diabetes model has been characterized in detail.[11–13]

Working Heart Perfusion Protocols

Rats (14 weeks) were anesthetized with pentobarbital (150 $mg \cdot kg^{-1}$, intraperitoneally). Each heart was rapidly removed and perfused initially in a nonworking Langendorff mode with Krebs-Henseleit solution containing 3% bovine serum albumin for 10 minutes, before establishing the working mode perfusion as previously described.[14] Left ventricular work ($mL \cdot min^{-1} \cdot mm\ Hg$) was calculated as left ventricular work · cardiac output × (aortic systolic pressure − preload). Measurements of mechanical function were averaged for the initial 30 minutes of aerobic perfusion (no insulin) and for the following 60 minutes of perfusion in the presence of insulin. Hearts were assigned to the following 6 groups (Supplemental Digital Content 1, which is a scheme detailing the protocols, http://links.lww.com/AA/B32). Groups 1 and 2: untreated healthy or diabetic hearts perfused without insulin for 30 minutes followed by 60 minutes with insulin; groups 3 and 4: healthy or diabetic hearts perfused without insulin for 30 minutes and then treated with insulin plus 10 μM propofol (Diprivan); and groups 5 and 6 (solvent controls): healthy or diabetic hearts perfused without insulin for 30 minutes and then treated with insulin plus Intralipid (25 μM, as corresponding solvent control of Diprivan). Ten micromolar propofol (Diprivan) was chosen because this concentration reflects the effect-site concentration at which loss of consciousness occurs in humans.[15] Because the heart perfusate contained 3% bovine serum albumin, some of the administered propofol was likely bound, thereby reducing the free active concentration as occurs under clinical conditions. Additional healthy and diabetic hearts were perfused for 90 minutes without insulin or for 30 minutes only in the absence of insulin (required for the measurement of glucose uptake).

Metabolic Flux Measurements of Glycolysis

The rate of glycolysis was determined by perfusing hearts with [5-^{3}H]glucose.[16] Total myocardial ^3H_2O production (liberated from [5-^{3}H]glucose at the enolase step of glycolysis) was determined every 10 minutes and the rates were expressed as $\mu mol \cdot gdw^{-1} \cdot min^{-1}$.

Determination of Tissue Glycogen Content and [5-^{3}H]glucose Incorporation

Glycogen content (μmol glucosyl units per gdw) and the incorporation of [5-^{3}H]glucose into glycogen were also determined for each heart.[14,16]

Glucose Uptake in Perfused Working Hearts

Glucose uptake (in $\mu mol \cdot gdw^{-1} \cdot min^{-1}$) was calculated based on its metabolism by glycolysis and its incorporation into glycogen. The average rate of glucose uptake in the 30 to 90 minutes treatment period is the sum of the rate of glycolysis and the rate of glycogen synthesis. Glycogen synthesis in the 30 to 90 minutes treatment period is calculated from the increase in radiolabeled glycogen content (calculated as the difference between radiolabeled contents at 30 and 90 minutes).

Citrate Synthase Activity (Oxidative Capacity)

The activity of the mitochondrial matrix marker enzyme citrate synthase was measured at 412 nm by monitoring the formation of thionitrobenzoate, as previously described.[17]

Determination of Glycolytic Metabolites

Heart tissue (75 mg) was deproteinized with perchloric acid and supernatants were adjusted to pH 3.5 using K_2CO_3 (5 M). Glucose-6-phosphate, fructose-6-phosphate, and fructose-1,6-bisphosphate contents in heart tissue ($nmol \cdot gdw^{-1}$) were determined by a coupled enzymatic assay, as described previously.[18]

Immunoblotting

Total tissue homogenates were prepared from frozen heart tissue homogenized in ice-cold buffer containing 50 mM

Tris (pH 8.0), 150 mM NaCl, and 1% Nonidet P-40, supplemented with protease and phosphatase inhibitors, as previously described.[14] Membrane and cytosolic fractions were prepared according to the methods reported by Lizotte et al.[19] Protein concentration was measured by Bradford assay. Densitometric analysis of immunoblots was performed using ImageJ software.[a] The following proteins were probed with the appropriate antibodies from Cell Signaling Technology (unless otherwise stated; Cell Signaling Technology, Inc., Danvers, MA): phospho-Akt (Ser473 and Thr308), Akt, phospho-GSK3β (Ser9), GSK3β, phospho-AMPK (Thr172), AMPK, phospho-ERK1/2 (Thr202/Tyr204), Erk1/2, phospho-p38MAPK (Thr180/Tyr182), p38MAPK, phospho-JNK (Thr183/Tyr185; Millipore, Billerica, MA), JNK (Millipore), phospho-S6K1 (Thr389; Abcam, Cambridge, MA), S6K1 (Abcam), insulin receptor substrate-1 (IRS-1), phospho-IRS-1 (Ser1100/h1101, Ser307/h312), phospho-IRS-1 (Tyr608/h612; Abcam), GLUT4, protein kinase Cθ (PKCθ), and protein kinase $C\beta_{II}$ ($PKC\beta_{II}$) (Santa Cruz Biotechnology, Dallas, TX). Because $PKC\beta_{II}$ persistently translocates to the membrane under insulin stimulation,[20] it was measured in membrane fractions. Tubulin (Santa Cruz Biotechnology, Santa Cruz, CA) was used as loading control in blots where total tissue extracts or cytosolic fractions were used. GLUT4, PKCθ, and $PKC\beta_{II}$ were normalized to the membrane marker Na^+/K^+-ATPase, which showed no difference in the expression between healthy and type-2 diabetic rat hearts (not shown). Immunoblots for the treatment groups (insulin, insulin plus Diprivan, and insulin plus Intralipid) were run within the same gel for each model (healthy or diabetic hearts). Samples of the same healthy and diabetic hearts with insulin treatment only were further run on additional gels to gauge the relative intensity levels of each protein of interest to allow direct comparisons between models.

Mass Spectrometry for Acylcarnitine Profiling of Cardiac Tissue

Tissue levels of 32 acylcarnitine species were measured using electrospray ionization tandem mass spectrometry, as described previously.[14]

Mass Spectrometry for the Determination of Phospholipids in Cardiac Tissue

Liquid chromatography-tandem mass spectrometry combining high-performance liquid chromatography separation on normal-phase column with multiple parent-ion or neutral loss scans on a triple-quadruple mass spectrometer was used to analyze the following phospholipid classes from lipid extracts of cardiac tissues.[21] The following species were determined: sphingomyelin, phosphatidylcholine, phosphatidylglycerol, phosphatidylethanolamine, phosphatidic acid, and ceramides. Supplemental Digital Content 2 contains detailed protocols (http://links.lww.com/AA/B33).

Mass Spectrometry for the Determination of Sphingoid Bases in Cardiac Tissue

The profile of backbone sphingoid bases was determined after hydrolysis, as previously described (Supplemental Digital Content 2, http://links.lww.com/AA/B33).[22] The sphingoid bases analyzed included C16-sphingosine, C16-sphinganine, C17-sphingosine, C18-sphingosine, C18-sphinganine, C20-sphingosine, C18-sphingadiene, deoxysphinganine, and deoxysphingosine. Software tools for quantitative analysis of mass spectrometric lipidome data were used.[23]

Statistical Analysis

Values are given as mean (SD) or median (25th, 75th percentile) depending on the underlying data distribution for the indicated number of independent observations. A sample size of 5 for changes in glucose uptake was calculated based on published data on insulin-induced cardiac glucose uptake.[24,25] With an expected difference of 1.5 μmol glucose·gdw^{-1}·min^{-1}, an SD of 0.6 μmol glucose·gdw^{-1}·min^{-1}, an α level of 0.05, and a power of 0.8, a minimal sample size of 5 was calculated. Additional hearts were enrolled to account for the intrinsic reduced insulin responsiveness of the diabetic heart. The significance of differences in hemodynamic and metabolic (glycolysis rates) variables among groups was determined by 2-way repeated-measures analysis of variance (ANOVA) followed by an all pairwise multiple comparison procedure using the Holm-Sidak method for post hoc analysis. Differences were evaluated by Student *t* test (2 groups) or by ANOVA followed by an all pairwise multiple comparison procedure using the Holm-Sidak method for post hoc analysis. Nonparametric methods (Kruskal-Wallis ANOVA on ranks) were used in the case where the conditions for parametric ANOVA were not met (i.e., equal variance and normally distributed residuals). Normality was assessed using the Shapiro-Wilk test, whereas equal variance was assessed using the Levene test (the default *P* value of 0.05 to reject was used in both cases). Differences are considered significant if the overall $P < 0.05$. SigmaPlot (version 12.0; Systat Software, Inc., Chicago, IL) was used for the analyses.

RESULTS

After 6 weeks of fructose feeding, rats exhibited total body insulin resistance. Glucose tolerance tests showed delayed glucose clearance with markedly increased blood glucose levels compared with healthy rats (Supplemental Digital Content 3, which shows glucose tolerance and insulin sensitivity tests, http://links.lww.com/AA/B34). An intraperitoneal insulin challenge resulted in a less prominent blood glucose reduction in the fructose-fed diabetic rats compared with that in healthy rats (Supplemental Digital Content 3, http://links.lww.com/AA/B34). We have previously shown that these rats also show increased fasting glucose, triglyceride, and insulin blood levels, the classical features of type-2 diabetes mellitus.[11] Furthermore, during working mode perfusion, the hearts of diabetic rats exhibited a reduced insulin-stimulated glucose uptake rate (1.4 ± 0.6 vs 2.4 ± 0.4 μmol·gdw^{-1}·min^{-1}; $P = 0.002$) (Fig. 1A), consistent with cardiac insulin resistance. Diabetic hearts also had higher levels of triglycerides, lysophosphatidylcholine, and lysophosphatidylethanolamine and lower mitochondrial content and dysfunctional β-oxidation with increased tissue concentrations of acylcarnitines compared with hearts from age-matched healthy rats (Table 1).

[a]Available at: http://rsbweb.nih.gov/ij/. Accessed December 1, 2008.

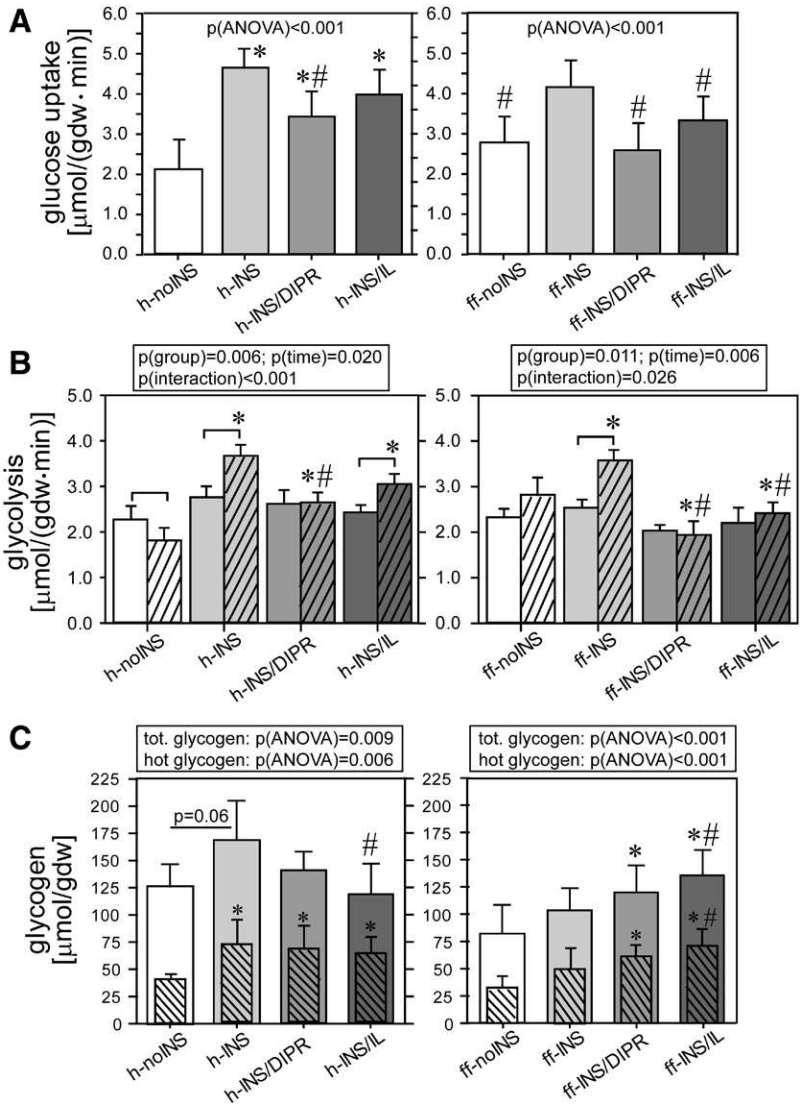

Figure 1. Glucose uptake, glycolysis, and glycogen metabolism. A, Glucose uptake was calculated from glycolytic flux and glycogen synthesis over 60 minutes in all groups. B, Average rates of glycolysis without insulin (first 30 minutes) and with insulin (subsequent 60 minutes, hatched bars). Horizontal brackets indicate significant differences for factor "time." C, Total and radiolabeled (hatched bars) glycogen tissue content at the end of perfusions. gdw = gram dry heart weight; h = healthy; ff = fructose-fed; noINS = perfusion without insulin; INS = insulin alone; INS/DIPR = perfusion with insulin and treated with Diprivan (10 µM); INS/IL = perfusion with insulin treated with Intralipid (25 µM); ANOVA = analysis of variance. *N* = 6–10 for each group. *Versus corresponding noINS group. #Versus corresponding INS group.

Diprivan and Intralipid Reduce Glucose Uptake and Redirect Glucose to Glycogen Stores in Insulin-Stimulated Type-2 Diabetic Hearts

To evaluate the effects of Diprivan and Intralipid on the insulin response, Diprivan and Intralipid were added to the perfusate 3 minutes before insulin administration. In accordance with previous reports in rat hearts,[26,27] insulin administration was accompanied with mild negative inotropic effects (Table 2). Intralipid reduced glucose uptake in both healthy and diabetic hearts by 25% and 61% of insulin response on average, respectively (Fig. 1A). Likewise, Diprivan reduced glucose uptake to a greater extent in both healthy and diabetic hearts by 48% and 109% of the insulin response, respectively (Fig. 1A). The reduced glucose uptake in Diprivan-treated healthy hearts and Diprivan-treated and Intralipid-treated diabetic hearts was due to a reduction in glycolytic flux rates (Fig. 1B). In insulin-stimulated healthy hearts, the treatment with both fat emulsions decreased total glycogen content (Fig. 1C), with the most profound effect occurring in the Intralipid group (h-INS versus h-INS/IL post hoc; $P = 0.008$). Conversely, glycogen levels increased in diabetic hearts (Fig. 1C), again with the largest effect occurring in the Intralipid group (ff-INS versus ff-INS/IL post hoc; $P = 0.043$). Consistent with reduced oxidative capacity in diabetic hearts, as measured by citrate synthase activity (Table 1), glucose was diverted from substrate oxidation to glycogen storage when exposed to fat emulsions. Together, these data show that Diprivan and Intralipid promote insulin resistance, predominantly in diabetic hearts.

Diprivan and Intralipid Impair GLUT4 Trafficking in Insulin-Stimulated Type-2 Diabetic Hearts and Propofol Specifically Increases Phosphorylation of IRS-1 at Ser1100

GLUT4 protein content was reduced in insulin-stimulated diabetic hearts (Panel A in Supplemental Digital Content 4, which shows differences in protein expression and phosphorylation of insulin-stimulated healthy and diabetic hearts, http://links.lww.com/AA/B35), but membrane translocation was largely maintained (data not shown). When comparing the effect of Diprivan and Intralipid on GLUT4 trafficking to the sarcolemma in the healthy hearts, there was a clear propofol-specific impairment (Fig. 2A). GLUT4 translocation to the membrane was also reduced

Table 1. Characteristics of Healthy and Diabetic Hearts

	H	ff	*P*	Mean difference (CI)
Citrate synthase activity (μmol mL^{-1} min^{-1} μg^{-1})	20.2 (2.1)	16.9 (3.1)	**<0.001**	3.3 (2.2–4.5)
Cardiac tissue triglycerides (μmol gdw^{-1})	6.35 (2.01)	7.74 (2.29)	**0.016**	−1.39 (−2.52 to −0.27)
Cardiac tissue levels of phospholipids				
Lysophosphatidylcholine (nmol mg^{-1})	151 (18)	198 (19)	**0.019**	−48 (−83 to −12)
Lysophosphatidylethanolamine (nmol mg^{-1})	129 (27)	197 (27)	**0.012**	−68 (−115 to −21)
Phosphatidylethanolamine (nmol mg^{-1})	50 (8)	66 (14)	0.119	−16 (−36 to 6)
Sphingomyelin (nmol mg^{-1})	34.7 (6.8)	33.1 (8.5)	0.780	1.6 (−11.7 to 14.9)
Cardiac tissue levels of sphingolipids				
C16-sphingosine (pmol per 100 μg)	0.56 (0.14)	0.53 (0.08)	0.737	0.03 (−0.17 to 0.22)
C18-sphingosine (pmol per 100 μg)	154 (21)	152 (29)	0.917	2 (−42 to 46)
C18-sphinganine (pmol per 100 μg)	1.7 (0.3)	1.4 (0.2)	0.075	0.3 (−0.05 to 0.77)
C18-sphingadiene (pmol per 100 μg)	41 (11)	40 (9)	0.924	1 (−17 to 18)
C20-sphingosine (pmol per 100 μg)	0.35 (0.10)	0.50 (0.08)	0.057	−0.15 (−0.31 to 0.006)
Cardiac tissue levels of acylcarnitines				
Free carnitine (C0; nmol g^{-1})	441 (38)	492 (71)	0.207	−51 (−139 to 36)
Total acylcarnitines (nmol g^{-1})	393 (86)	557 (44)	**0.011**	−164 (−276 to −51)
Acetylcarnitine (C2; nmol g^{-1})	351 (86)	491 (30)	**0.018**	−140 (−247 to −32)
Short-chain acylcarnitines (nmol g^{-1})	359 (86)	502 (32)	**0.017**	−143 (−252 to −34)
Medium-chain acylcarnitines (nmol g^{-1})	0.97 (0.09)	1.42 (0.46)	0.070	−0.45 (−0.94 to 0.05)
Long-chain acylcarnitines (nmol g^{-1})	33 (4)	53 (14)	**0.016**	−20 (−35 to −5)

Data are presented as mean (SD). Acylcarnitine tissue levels are presented as total acylcarnitines, short-chain (C2–C6), medium-chain (C8–C12), and long-chain (C14 and higher) acylcarnitines. *N* = 44 (citrate synthase activity); *N* = 30 (tissue triglycerides); and *N* = 5–6 (sphingolipids/acylcarnitines).
CI = confidence interval; ff = rats fed standard chow and 10% fructose added to the drinking water for 6 weeks; gdw = gram dry heart weight; h = age-matched healthy control rats (fed standard chow and water).

Table 2. Cardiac Function in Perfused Healthy and Diabetic Hearts

		h-noINS	h-INS	h-INS/DIPR	h-INS/IL	ff-noINS	ff-INS	ff-INS/DIPR	ff-INS/IL
HR (min^{-1})	Equilibration	241 (24)	262 (19)	256 (23)	252 (12)	229 (11)	228 (10)	232 (27)	229 (17)
	Treatment	251 (28)	264 (17)	252 (34)	245 (13)	230 (15)	224 (16)	230 (22)	234 (10)
RM-ANOVA *P* (group); *P* (time); *P* (interaction)			0.36; 0.87; 0.12				0.92; 0.93; 0.22		
CO ($mL \cdot min^{-1}$)	Equilibration	66 (8)	67 (6)	65 (6)	69 (7)	65 (4)	67 (9)	66 (11)	63 (11)
	Treatment	66 (7)	61 (9)[a]	66 (8)	65 (6)[a]	61 (6)	58 (13)[a]	64 (11)	62 (14)
RM-ANOVA *P* (group); *P* (time); *P* (interaction)			0.86; **0.004**; **0.023**				0.95; **0.010**; 0.06		
LVW (mm Hg · L min^{-1})	Equilibration	7.95 (1.20)	7.97 (1.06)	7.92 (0.79)	8.19 (1.30)	8.19 (1.34)	8.36 (1.42)	8.58 (1.65)	7.80 (1.46)
	Treatment	7.78 (1.09)	6.91 (1.37)[a]	7.58 (1.11)	7.54 (1.17)[a]	7.59 (1.13)	7.09 (1.98)[a]	8.40 (1.68)	7.72 (1.61)
RM-ANOVA *P* (group); *P* (time); *P* (interaction)			0.83; **<0.001**; 0.08				0.76; **0.002; 0.035**		

Data are presented as mean (SD). Two-way RM-ANOVA was performed to compare the following 4 groups of hearts from healthy (h) and from fructose-fed (ff) rats, namely noINS, INS, INS/DIPR, and INS/IL. It was followed by multiple comparison procedures (Holm-Sidak method).
HR = heart rate; CO = cardiac output; LVW = left ventricular work; RM-ANOVA = repeated-measures analysis of variance; noINS = control group (time-matched perfusion without insulin; *n* = 7); INS = insulin-only group (*n* = 9); INS/DIPR = insulin plus Diprivan (10 μM; *n* = 7); INS\IL = insulin plus Intralipid (*n* = 7).
[a]Significantly different from corresponding baseline value.

in Diprivan-treated and Intralipid-treated diabetic hearts (Fig. 2A). This was consistent with reduced glycolysis and glucose uptake, as measured with the radioactive tracer in the respective groups. The analysis of the glycolytic metabolites further revealed that only Diprivan reduced phosphofructokinase-1 activity in diabetic but not in healthy hearts (Supplemental Digital Content 5, a table showing glycolytic metabolites, http://links.lww.com/AA/B36). In terms of IRS-1 phosphorylation at Ser1100(h1101), there was also an evident propofol-specific effect in both healthy and diabetic hearts (Fig. 2B). Phosphorylation of IRS-1 at Ser307(h312) was already increased in diabetic hearts independent of any treatment (Fig. 2C, and Panel B in Supplemental Digital Content, http://links.lww.com/AA/B35). Phosphorylation of Tyr608(h612) of IRS-1 was similar between healthy and diabetic hearts and not affected by either treatments (Fig. 2D). There was no difference in the expression of IRS-1 between healthy and diabetic hearts (data not shown). Overall, propofol impairs GLUT4 trafficking and specifically increases serine phosphorylation of IRS-1. Intralipid impairs GLUT4 trafficking only in type-2 diabetic hearts.

Diprivan and Intralipid Elicit a Distinct Activity Pattern of Metabolic and Stress Kinases in Insulin-Stimulated Type-2 Diabetic Hearts

By comparing the pattern of metabolic kinase phosphorylation between Diprivan and Intralipid treatment in insulin-stimulated healthy hearts, we observed that propofol specifically increased Akt phosphorylation at Ser473 and Thr308 (Fig. 3, A and B). Diprivan and Intralipid similarly enhanced GSK3β phosphorylation (Fig. 3C), but neither treatment had any effect on AMPK phosphorylation (Fig. 3D) nor any of the stress kinases tested (Fig. 4). However, in diabetic hearts, neither Diprivan nor Intralipid affected Akt phosphorylation at Ser473 or Thr308. GSK3β and AMPK phosphorylation were similarly enhanced by both Diprivan

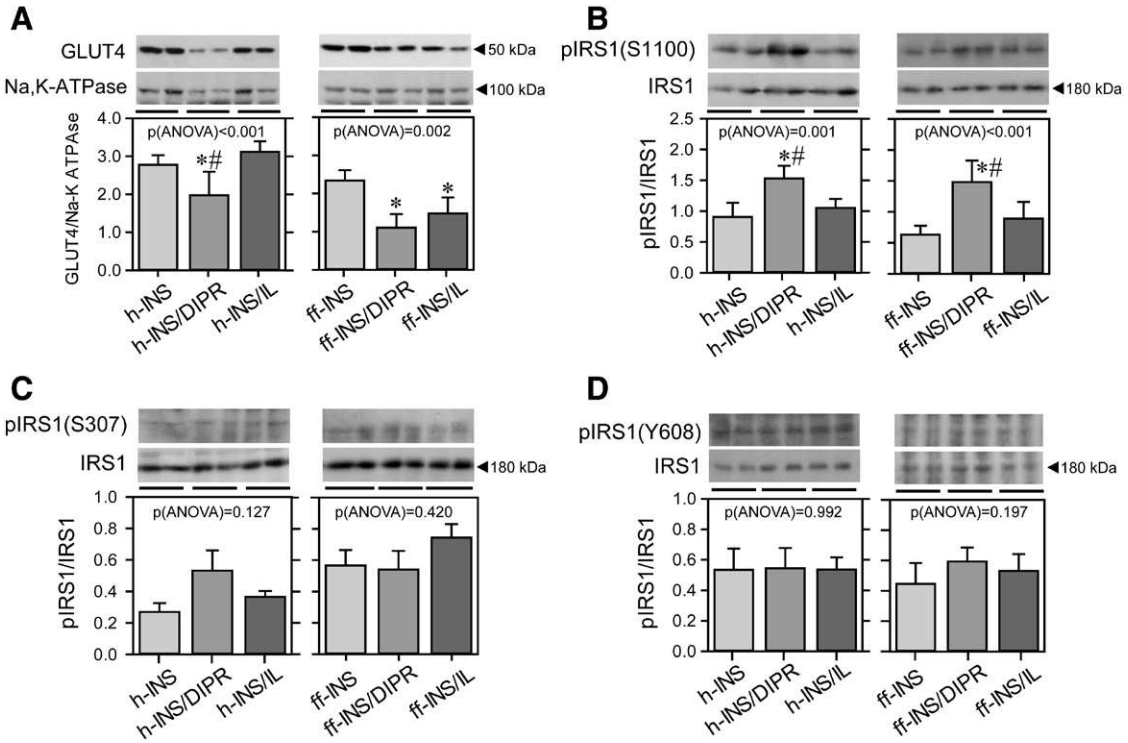

Figure 2. GLUT4 trafficking and insulin receptor substrate-1 (IRS-1) phosphorylation in insulin-stimulated healthy and diabetic hearts. A, GLUT4 in membrane fractions. GLUT4 levels were normalized to Na^+/K^+-ATPase. B–D, IRS-1 phosphorylation at Ser1100, Ser307, and Tyr608. INS = insulin alone; INS/DIPR = perfusion with insulin and treated with Diprivan (10 μM); INS/IL = perfusion with insulin and treated with Intralipid (25 μM); h = healthy; ff = fructose-fed; ANOVA = analysis of variance. *N* = 4–5 for each group. *Versus INS. #Versus INS/IL.

and Intralipid treatment in diabetic hearts (Fig. 3, C and D). Diprivan and Intralipid treatment further activated ERK1/2 exclusively in diabetic hearts (Fig. 4A). Only Diprivan activated p38MAPK and S6K1 in diabetic hearts (Fig. 4, B and C). Expression of JNK was increased in diabetic hearts (Panel C in Supplemental Digital Content 3, http://links.lww.com/AA/B34), but there was no difference in phosphorylation in response to Diprivan or Intralipid treatment (Fig. 4D). Membrane and total tissue expression of the novel PKCθ was increased in diabetic hearts (Panel D in Supplemental Digital Content 3, http://links.lww.com/AA/B34). Only Diprivan significantly increased PKCθ translocation to the membrane in healthy hearts (Fig. 5A). The conventional $PKC\beta_{II}$ was activated only in Diprivan-treated healthy and diabetic hearts (Fig. 5B). PKC activation by Diprivan only clearly indicates a propofol-specific effect. There was no increase in total expression of Akt, GSK3β, AMPK, ERK1/2, p38MAPK, S6K1, and $PKC\beta_{II}$ in diabetic hearts compared with healthy hearts (data not shown). Likewise, there was no change in phosphorylation of Akt, GSK3β, AMPK, ERK1/2, p38MAPK, and S6K1.

Diprivan and Intralipid Promote Accumulation of Potentially Diabetogenic Fatty Acid Intermediates in Insulin-Stimulated Type-2 Diabetic Hearts

To determine whether diabetic hearts exposed to Diprivan or Intralipid showed changes in concentrations of potentially toxic lipid species, we examined the concentrations of phospholipids and sphingolipids in cardiac tissue extracts using mass spectrometry. These measurements showed accumulation of the phospholipids phosphatidylglycerol and phosphatidylethanolamine in Diprivan-treated and Intralipid-treated diabetic hearts (Table 3). Unexpectedly, only Diprivan but not Intralipid reduced ceramide levels in diabetic hearts. In healthy hearts, both Diprivan and Intralipid reduced phosphatidylethanolamine, the most abundant sphingoid base C18-sphingosine, and its saturated counterpart C18-sphinganine (Table 3). Diprivan was more effective than Intralipid in increasing C18-sphingosines and sphingadienes in diabetic hearts.

DISCUSSION

Fatty acids and fat emulsions impair glucose metabolism via the Randle cycle[28] and hence are used in experimental settings to generate insulin resistance. In otherwise healthy volunteers, infusion of long-chain triglycerides reduces insulin sensitivity.[29] Nonetheless, fat emulsions are widely used in surgical patients either as a solvent for the IV anesthetic, propofol, or in vulnerable intensive care unit patients for sedation or parenteral nutrition. However, not much is known as to how fat emulsions or propofol itself affects glucose metabolism in the heart. In our experiments, we used type-2 diabetic hearts to establish the impact of propofol (Diprivan) and its solvent, Intralipid, on insulin-induced glucose uptake. Consistent with previous reports,[30] we show that the early diabetic heart already exhibits accumulation of triglycerides, dysfunctional β-oxidation, and reduced oxidative capacity. Our discovery that Intralipid and propofol in the formulation of Diprivan worsen lipid overload

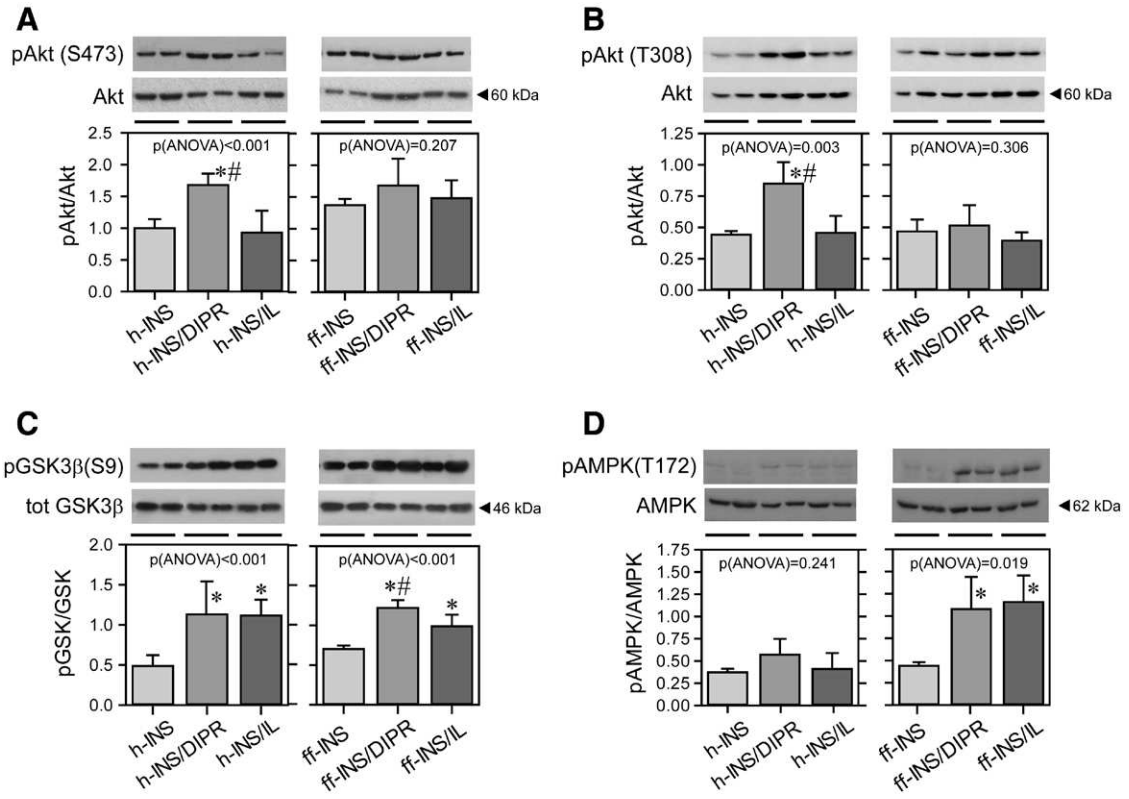

Figure 3. Activation pattern of metabolic kinases in insulin-stimulated healthy and diabetic hearts. A, Akt phosphorylation at Ser473. B, Akt phosphorylation at Thr308. C, GSK3β phosphorylation at Ser9. D, AMPK phosphorylation at Thr172. INS = insulin alone; INS/DIPR = perfusion with insulin and treated with Diprivan (10 μM); INS/IL = perfusion with insulin and treated with Intralipid (25 μM); h = healthy; ff = fructose-fed; ANOVA = analysis of variance. *N* = 4–5 for each group. *Versus INS. #Versus INS/IL.

and further impair glucose metabolism in these hearts is novel but in line with current knowledge on lipotoxicity and associated inflammation in the diabetic heart.[1,31–33]

Our study shows the following salient findings. First, insulin-stimulated glucose uptake was reduced in Diprivan-treated healthy hearts, and the reduction in glucose uptake under Intralipid treatment almost reached statistical significance ($P = 0.078$). However, only Diprivan abolished the action of insulin on glycolytic flux. This was accompanied by impaired GLUT4 trafficking to the sarcolemma. Conversely, healthy hearts responded to insulin in the presence of Intralipid and increased glycolytic flux, implying that Intralipid alone only marginally affects insulin sensitivity.[28] Possibly, the release of intracellular glucose stores from glycogen due to unsaturated fatty acid–induced activation of glycogen phosphorylase[34] caused the reduction in glucose uptake without changing GLUT4 trafficking. Glycerol, another constituent of Intralipid, may have further contributed to pyruvate formation and thus reduced glucose uptake.[35] Together, these results indicate that propofol itself acutely promotes insulin resistance in healthy hearts. This conclusion is also supported by our observation that Diprivan, but not Intralipid, caused marked activation and membrane translocation of PKCθ and PKCβII as well as the phosphorylation at Ser1100(h1101) of the IRS protein IRS-1, a key player in insulin signaling.[36,37] More recently, insulin resistance and feedback inhibition of insulin signaling were found to be mediated by serine/threonine phosphorylation of IRS-1.[36,37] There are as many as 50 serine phosphorylation sites of IRS-1 and most of them negatively modulate insulin effects, whereas multiple (so far at least 8) tyrosine phosphorylation sites of IRS-1 have opposite effects.[37] Ser1100(h1101) of IRS-1 is a target of PKCθ,[38] the importance of which in insulin signaling is further supported by studies showing the lack of insulin resistance to dietary challenge in PKCθ-knockout mice.[39,40] Overexpression of $PKC\beta_{II}$ in mouse skeletal muscle induces insulin resistance.[41] Both PKC isoforms further inhibit insulin receptor tyrosine kinase by serine phosphorylation.[42] Interestingly, healthy hearts exposed to Diprivan showed increased Akt phosphorylation at Ser473 and Thr308, consistent with full Akt activation. It appears that Akt signaling in Diprivan-treated healthy hearts is dysfunctional. However, it inhibits phosphatases,[43] and it has been reported that sustained phosphorylation of Akt mediates insulin-induced feedback inhibition[44] and thus contributes to cardiac insulin resistance.[45]

Second, both Diprivan and Intralipid abolished the action of insulin on glycolytic flux in early diabetic hearts and impaired GLUT4 trafficking to the sarcolemma. In addition, Diprivan decreased phosphofructokinase-1 activity in these hearts. The reduced insulin sensitivity in diabetic hearts exposed to Diprivan and Intralipid was closely linked to increased phosphorylation of AMPK and stress kinases (ERK1/2 and p38MAPK). Insulin inhibits cardiac AMPK, and hearts perfused in the absence of insulin have been reported to show higher AMPK phosphorylation than hearts perfused in the presence of insulin.[46] In fact, phosphorylation of AMPK at Ser485 or Ser491 is responsible for the

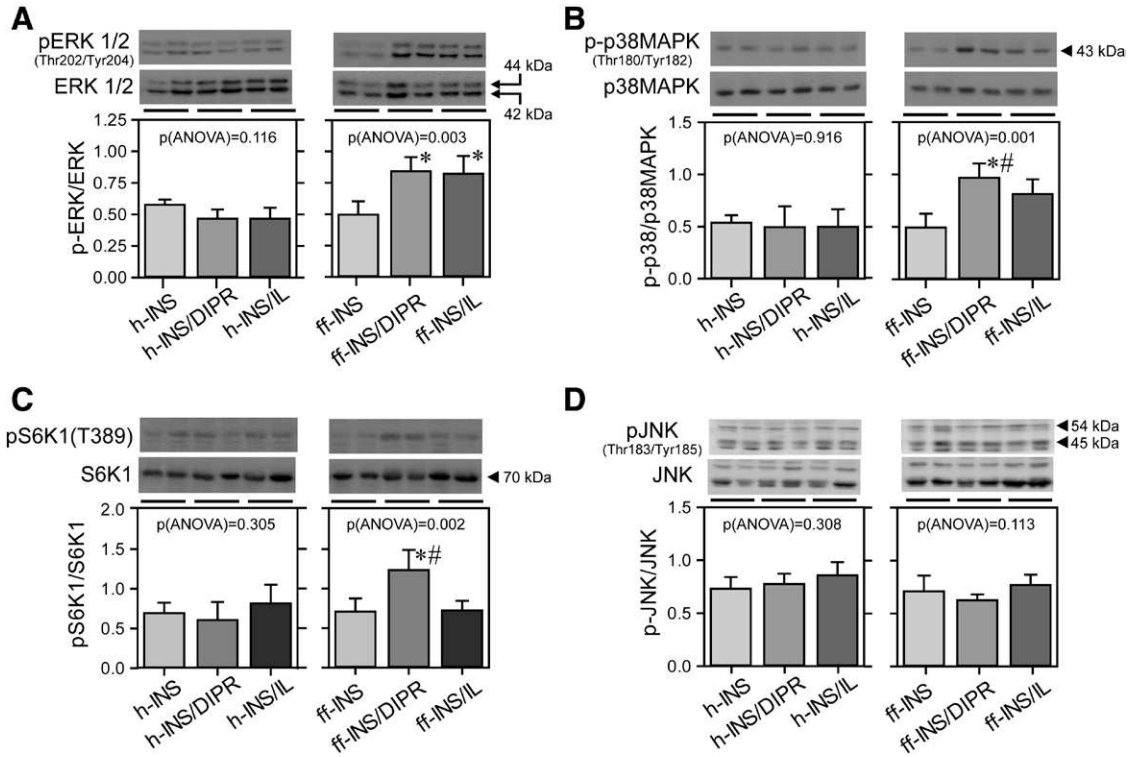

Figure 4. Activation pattern of stress kinases in insulin-stimulated healthy and diabetic hearts. A, ERK1/2 phosphorylation at Thr202/Tyr204. B, p38MAPK phosphorylation at Thr180/Tyr182. C, S6K1 phosphorylation at Thr389. D, JNK phosphorylation at Thr183/Tyr185. INS = insulin alone; INS/DIPR = perfusion with insulin and treated with Diprivan (10 μM); INS/IL = perfusion with insulin and treated with Intralipid (25 μM); h = healthy; ff = fructose-fed; ANOVA = analysis of variance. *N* = 4–5 for each group. *Versus INS. #Versus INS/IL.

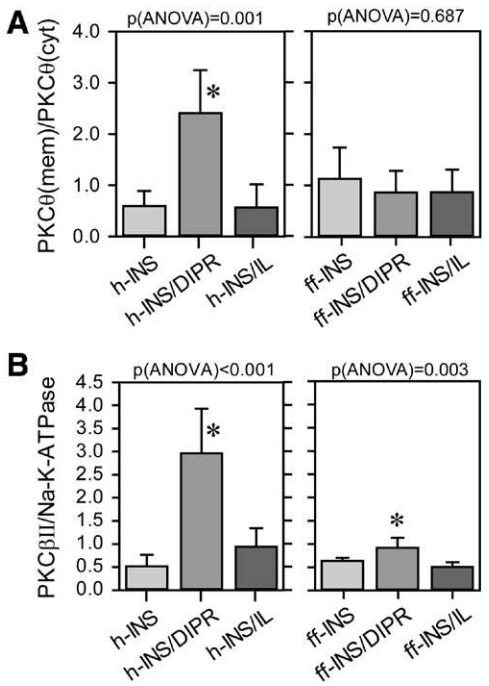

Figure 5. Protein kinase C (PKC) activation in insulin-stimulated healthy and diabetic hearts. A, Translocation of novel PKCθ as measured by membrane-to-cytosolic ratio. B, Conventional $PKC\beta_{II}$ protein levels in the membrane fraction. INS = insulin alone; INS/DIPR = perfusion with insulin and treated with Diprivan (10 μM); INS/IL = perfusion with insulin and treated with Intralipid (25 μM); h = healthy; ff = fructose-fed; ANOVA = analysis of variance. *N* = 4–5 for each group. *Versus INS. #Versus INS/IL.

effect of high insulin concentrations to blunt AMPK activation (Thr172 site) in the heart.[47] Our data are thus consistent with the concept that activation of AMPK ensures adequate cardiac energy production when glucose utilization is compromised.[48] AMPK also inhibits insulin signalling by phosphorylating IRS-1 at Ser789(h794).[49] Diprivan-mediated and Intralipid-mediated insulin resistance and AMPK activation may have also lead to the observed accumulation of glycogen in diabetic hearts.[50] Consistent with this interpretation, glycogen synthase kinase-3β phosphorylation was increased in Diprivan-treated and Intralipid-treated diabetic hearts leading to the activation of glycogen synthase. Finally, increased ERK1/2 and p38MAPK activities also inhibit IRS-1 by phosphorylation at Ser612 (ERK1/2)[37,51] and Ser636 (p38MAPK),[52] respectively. In diabetic hearts, only Diprivan treatment activated PKCβII and the pro-inflammatory S6K1, which also promotes Ser1100(h1101) phosphorylation of IRS-1,[53] again implying distinct diabetogenic effects of propofol itself.

Third, our study shows for the first time that administration of Diprivan and Intralipid leads to accumulation of potentially diabetogenic lipids in the heart. A recent study found that prediabetes and type-2 diabetes are associated with increased plasma levels of phosphatidylethanolamine, phosphatidylglycerol, and ceramides.[54] Lysophosphatidylcholine, another phospholipid, is reportedly an efficient effector of fatty acid–induced insulin resistance.[55] Lysophosphatidylcholine activates JNK, which phosphorylates IRS-1 at Ser307(h312). Moreover, the increased levels of phosphatidylethanolamine detected in

Table 3. Phospholipids and Sphingolipids in Perfused Healthy and Diabetic Hearts

	h-INS	h-INS/DIPR	h-INS/IL	ff-INS	ff-INS/DIPR	ff-INS/IL
Phospholipids						
Phosphatidylethanolamine (nmol · mg^{-1})	60 (11)	45 (6)[a]	46 (8)[a]	48 (11)	71 (14)[a]	65 (13)[a]
P	**0.015**			**0.009**		
Lysophosphatidylcholine (nmol · mg^{-1})	68 (32)	84 (34)	67 (25)	108 (43)	143 (49)	120 (29)
P	0.524			0.308		
Lysophosphatidylethanolamine (nmol · mg^{-1})	89 (68)	53 (31)	47 (21)	62 (29)	75 (30)	102 (41)
P	0.213			0.106		
Phosphatidylglycerol (nmol · mg^{-1})	4.0 (1.1)	4.0 (2.1)	3.1 (2.4)	3.1 (0.6)	4.5 (1.0)[a]	4.5 (1.4)[a]
P	0.674			**0.025**		
Sphingomyelin (nmol · mg^{-1})	38 (8)	29 (5)	31 (11)	25 (5)	29 (6)	28 (5)
P	0.140			0.262		
Ceramides (nmol · mg^{-1})	1.4 (0.4; 2.7)	2.2 (0.7; 4.5)	NA	4.1 (2.2)	1.3 (1.3)[b]	4.4 (1.9)
P		NA		**0.021**		
Sphingoid bases						
C16SO (pmol per 100 μg)	0.7 (0.1)	0.8 (0.1)	0.7 (0.1)	0.6 (0.1)	0.6 (0.1)	0.5 (0.1)
P	0.209			0.05		
C17SO (pmol per 100 μg)	2.3 (0.2)	2.0 (0.2)	2.0 (0.3)	1.4 (0.2)	1.6 (0.3)	1.6 (0.4)
P	0.072			0.544		
C18SO (pmol per 100 μg)	162 (13)	123 (12)[a]	134 (17)[a]	109 (10)	148 (17)[ab]	132 (14)[a]
P	**<0.001**			**<0.001**		
C18SA-diene (pmol per 100 μg)	41 (5)	38 (5)	36 (4)	29 (5)	47 (10)[a]	38 (7)[a]
P	0.137			**0.001**		
C18SA (pmol per 100 μg)	2.4 (0.4)	1.5 (0.2)[a,b]	1.9 (0.2)[a]	1.4 (0.2)	1.6 (0.3)	1.4 (0.2)
P	**<0.001**			0.338		
C20SO (pmol per 100 μg)	0.3 (0.06)	0.5 (0.1)[b]	0.3 (0.06)	0.4 (0.1)	0.3 (0.05)	0.3 (0.1)
P	**<0.001**			0.299		

Data are presented as mean (SD) or median (25th, 75th percentile). Analysis of variance was performed to compare INS, INS/DIPR, and INS/IL from healthy (h) and from fructose-fed (ff) rats. It was followed by a multiple comparison procedure (Holm-Sidak method). C16-sphinganine and the saturated and unsaturated deoxy-sphingoid bases were not detectable. $N = 7$ in all groups. Differences are considered significant (boldface) if the overall $P < 0.05$.

INS = insulin-only group; INS/DIPR = insulin plus Diprivan (10 μM); INS\IL = insulin plus Intralipid (25 μM); C16SO = C16-sphingosine (d16:1); C17SO = C17-sphingosine (d17:1); C18SO = C18-sphingosine (d18:1); C20SO = C20-sphingosine (d20:1); C18SA = C18-sphinganine (d18:0); C18SA-diene = sphingadiene (d18:2); NA = not available.

[a]Significantly different from INS.

[b]Significantly different from INS and INS/IL.

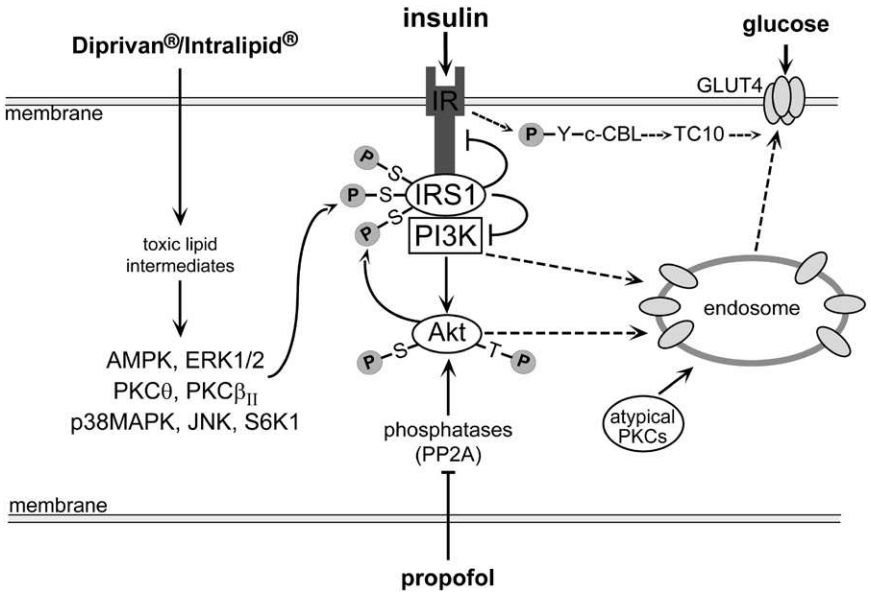

Figure 6. Working model of lipotoxicity by Diprivan and Intralipid in the heart. The diabetic heart is overloaded by fatty acid species and exhibits dysfunctional β-oxidation. Provision of supplementary fat or propofol to the diabetic myocardium raises levels of toxic lipids, which activate kinases mediating insulin resistance by hyperphosphorylation of the insulin receptor substrate-1 (IRS-1) at multiple serine/threonine residues. The hyperphosphorylated state of the IRS-1 reduces the activity of the insulin receptor (IR) tyrosine kinase and of phosphoinositide 3-kinase (PI3K). Reduced tyrosine kinase activity of the IR inhibits GLUT4 translocation via the Casitas b-lineage lymphoma (c-Cbl)-TC10 (a small GTPase) pathway (PI3K-independent), while reduced PI3K activity also reduces GLUT4 translocation. In contrast to conventional and novel PKC, atypical PKC promote GLUT4 trafficking. In healthy hearts, propofol persistently increases Akt activity possibly by inhibiting PP2A phosphatase activity,[43] which also provides feedback inhibition to the IRS-1 and reduces GLUT4 trafficking.

our study in the diabetic myocardium exposed to Diprivan and Intralipid may exert strong proinflammatory effects when oxidized or glycated.[56] Recent studies also linked increased plasma sphingolipid levels to impaired insulin signaling.[22]

Taken together, our data suggest that propofol and Intralipid activate key kinases involved in serine/threonine phosphorylation of IRS-1 and thereby reduce insulin signaling (Fig. 6). Increased serine phosphorylation of IRS-1 reduces GLUT4 trafficking either downstream via reduced phosphoinositide 3-kinase activation[45,57,58] or upstream via inhibition of insulin receptor tyrosine kinase activity,[59] which initiates small GTPase (TC10)–mediated phosphoinositide 3-kinase–independent GLUT4 exocytosis.[57]

Because insulin resistance is tightly associated with increased morbidity and mortality,[4–6] it is possible that further impairment of insulin signaling by Diprivan or Intralipid treatment in at-risk patients with diabetes may worsen clinical outcomes. A meta-analysis in surgical and critically ill patients reported higher complication rates in subgroups of patients treated with lipid-based parenteral nutrition compared with patients receiving lipid-free formulations.[60] Hence, future studies in at-risk patients are necessary to address the relevance of our experimental observations in the clinical setting.

In conclusion, our experiments show that Diprivan and Intralipid reduce glucose uptake predominantly in diabetic hearts. The loss of metabolic flexibility is triggered by alterations in insulin signaling and GLUT4 trafficking and accompanied by accumulation of potentially diabetogenic lipids.

ACKNOWLEDGMENTS

T. Hornemann and A. Zhakupova are grateful to the Center of Integrated Human Physiology (ZIHP) and the "radiz"–Rare Disease Initiative Zurich, Clinical Research Priority Program for Rare Diseases, University of Zurich.

DISCLOSURES

Name: Phing-How Lou, PhD.
Contribution: This author conducted most of the experiments, was involved in data analysis, and in writing the manuscript.
Attestation: Phing-How Lou has seen the original study data and approved the final manuscript.
Name: Eliana Lucchinetti, PhD.
Contribution: This author was involved in the design of the study, analyzed the data, and wrote the manuscript.
Attestation: Eliana Lucchinetti has seen and attests to the integrity of the original data and the analysis reported in this manuscript and is the archival author. Eliana Lucchinetti approved the final manuscript.
Name: Liyan Zhang, PhD.
Contribution: This author conducted some of the experiments.
Attestation: Liyan Zhang approved the final manuscript.
Name: Andreas Affolter, BSc.
Contribution: This author conducted some of the experiments.
Attestation: Andreas Affolter approved the final manuscript.
Name: Manoj Gandhi, PhD.
Contribution: This author conducted some of the experiments and was responsible for animal care.
Attestation: Manoj Gandhi approved the final manuscript.
Name: Assem Zhakupova, MS.
Contribution: This author conducted some of the experiments.
Attestation: Assem Zhakupova approved the final manuscript.
Name: Martin Hersberger, PhD.
Contribution: This author analyzed some of the data.
Attestation: Martin Hersberger approved the final manuscript.
Name: Thorsten Hornemann, PhD.
Contribution: This author performed some of the experiments and analyzed the data.
Attestation: Thorsten Hornemann approved the final manuscript.
Name: Alexander S. Clanachan, PhD.
Contribution: This author designed the study, analyzed the data, and wrote the manuscript.
Attestation: Alexander S. Clanachan approved the final manuscript.
Name: Michael Zaugg, MD, MBA, FRCPC.
Contribution: This author designed the study, analyzed the data, and wrote the manuscript.
Attestation: Michael Zaugg approved the final manuscript.
This manuscript was handled by: Markus W. Hollmann, MD, PhD.

REFERENCES

1. Park SY, Cho YR, Kim HJ, Higashimori T, Danton C, Lee MK, Dey A, Rothermel B, Kim YB, Kalinowski A, Russell KS, Kim JK. Unraveling the temporal pattern of diet-induced insulin resistance in individual organs and cardiac dysfunction in C57BL/6 mice. Diabetes 2005;54:3530–40
2. Voipio-Pulkki LM, Nuutila P, Knuuti MJ, Ruotsalainen U, Haaparanta M, Teräs M, Wegelius U, Koivisto VA. Heart and skeletal muscle glucose disposal in type 2 diabetic patients as determined by positron emission tomography. J Nucl Med 1993;34:2064–7
3. Morel S, Berthonneche C, Tanguy S, Toufektsian MC, Foulon T, de Lorgeril M, de Leiris J, Boucher F. Insulin resistance modifies plasma fatty acid distribution and decreases cardiac tolerance to in vivo ischaemia/reperfusion in rats. Clin Exp Pharmacol Physiol 2003;30:446–51
4. Lempiäinen P, Mykkänen L, Pyörälä K, Laakso M, Kuusisto J. Insulin resistance syndrome predicts coronary heart disease events in elderly nondiabetic men. Circulation 1999;100:123–8
5. Banerjee D, Biggs ML, Mercer L, Mukamal K, Kaplan R, Barzilay J, Kuller L, Kizer JR, Djousse L, Tracy R, Zieman S, Lloyd-Jones D, Siscovick D, Carnethon M. Insulin resistance and risk of incident heart failure: Cardiovascular Health Study. Circ Heart Fail 2013;6:364–70
6. Park HY, Kyeong-Ho, Park DS, Lee HS, Chang H, Kim YS, Cho KH. Correlation between insulin resistance and intracranial atherosclerosis in patients with ischemic stroke without diabetes. J Stroke Cerebrovasc Dis 2008;17:401–5
7. Sato K, Kitamura T, Kawamura G, Mori Y, Sato R, Araki Y, Yamada Y. Glucose use in fasted rats under sevoflurane anesthesia and propofol anesthesia. Anesth Analg 2013;117:627–33
8. Wanten GJ, Calder PC. Immune modulation by parenteral lipid emulsions. Am J Clin Nutr 2007;85:1171–84
9. Itani SI, Ruderman NB, Schmieder F, Boden G. Lipid-induced insulin resistance in human muscle is associated with changes in diacylglycerol, protein kinase C, and IkappaB-alpha. Diabetes 2002;51:2005–11
10. Crescenzo R, Bianco F, Coppola P, Mazzoli A, Valiante S, Liverini G, Iossa S. Adipose tissue remodeling in rats exhibiting fructose-induced obesity. Eur J Nutr 2014;53:413–19
11. Warren BE, Lou PH, Lucchinetti E, Zhang L, Clanachan AS, Affolter A, Hersberger M, Zaugg M, Lemieux H. Early mitochondrial dysfunction in glycolytic muscle, but not oxidative muscle, of the fructose-fed insulin-resistant rat. Am J Physiol Endocrinol Metab 2014;306:E658–67
12. Dai S, McNeill JH. Fructose-induced hypertension in rats is concentration- and duration-dependent. J Pharmacol Toxicol Methods 1995;33:101–7

13. Tran LT, Yuen VG, McNeill JH. The fructose-fed rat: a review on the mechanisms of fructose-induced insulin resistance and hypertension. Mol Cell Biochem 2009;332:145–59
14. Wang L, Ko KW, Lucchinetti E, Zhang L, Troxler H, Hersberger M, Omar MA, Posse de Chaves EI, Lopaschuk GD, Clanachan AS, Zaugg M. Metabolic profiling of hearts exposed to sevoflurane and propofol reveals distinct regulation of fatty acid and glucose oxidation: CD36 and pyruvate dehydrogenase as key regulators in anesthetic-induced fuel shift. Anesthesiology 2010;113:541–51
15. Kodaka M, Suzuki T, Maeyama A, Koyama K, Miyao H. Gender differences between predicted and measured propofol C(P50) for loss of consciousness. J Clin Anesth 2006;18:486–9
16. Omar MA, Fraser H, Clanachan AS. Ischemia-induced activation of AMPK does not increase glucose uptake in glycogen-replete isolated working rat hearts. Am J Physiol Heart Circ Physiol 2008;294:H1266–73
17. Srere PA. Citrate synthase. Methods Enzymol 1969;13:3–11
18. Omar MA, Verma S, Clanachan AS. Adenosine-mediated inhibition of 5′-AMP-activated protein kinase and p38 mitogen-activated protein kinase during reperfusion enhances recovery of left ventricular mechanical function. J Mol Cell Cardiol 2012;52:1308–18
19. Lizotte E, Tremblay A, Allen BG, Fiset C. Isolation and characterization of subcellular protein fractions from mouse heart. Anal Biochem 2005;345:47–54
20. Standaert ML, Avignon A, Arnold T, Saba-Siddique SI, Copper DR, Watson J, Zhou X, Galloway L, Farese RV. Insulin translocates PKC-epsilon and phorbol esters induce and persistently translocate PKC-beta 2 in BC3H-1 myocytes. Cell Signal 1996;8:313–6
21. Bligh EG, Dyer WJ. A rapid method of total lipid extraction and purification. Can J Biochem Physiol 1959;37:911–7
22. Othman A, Rütti MF, Ernst D, Saely CH, Rein P, Drexel H, Porretta-Serapiglia C, Lauria G, Bianchi R, von Eckardstein A, Hornemann T. Plasma deoxysphingolipids: a novel class of biomarkers for the metabolic syndrome? Diabetologia 2012;55:421–31
23. Haimi P, Uphoff A, Hermansson M, Somerharju P. Software tools for analysis of mass spectrometric lipidome data. Anal Chem 2006;78:8324–31
24. Folmes CD, Clanachan AS, Lopaschuk GD. Fatty acids attenuate insulin regulation of 5′-AMP-activated protein kinase and insulin cardioprotection after ischemia. Circ Res 2006;99:61–8
25. Gandhi M, Finegan BA, Clanachan AS. Role of glucose metabolism in the recovery of postischemic LV mechanical function: effects of insulin and other metabolic modulators. Am J Physiol Heart Circ Physiol 2008;294:H2576–86
26. Farah AE, Alousi AA. The actions of insulin on cardiac contractility. Life Sci 1981;29:975–1000
27. Svíglerová J, Kuncová J, Stengl M. Negative inotropic effect of insulin in papillary muscles from control and diabetic rats. Physiol Res 2005;54:661–70
28. Randle PJ, Garland PB, Hales CN, Newsholme EA. The glucose fatty-acid cycle. Its role in insulin sensitivity and the metabolic disturbances of diabetes mellitus. Lancet 1963;1:785–9
29. Rigalleau V, Beylot M, Pachiaudi C, Guillot C, Deleris G, Gin H. Mechanisms of glucose intolerance during triglyceride infusion. Am J Physiol 1998;275:E641–8
30. Gray S, Kim JK. New insights into insulin resistance in the diabetic heart. Trends Endocrinol Metab 2011;22:394–403
31. Goldberg IJ, Trent CM, Schulze PC. Lipid metabolism and toxicity in the heart. Cell Metab 2012;15:805–12
32. Palomer X, Salvadó L, Barroso E, Vázquez-Carrera M. An overview of the crosstalk between inflammatory processes and metabolic dysregulation during diabetic cardiomyopathy. Int J Cardiol 2013;168:3160–72
33. Ruberg FL. Myocardial lipid accumulation in the diabetic heart. Circulation 2007;116:1110–2
34. Gomez-Muñoz A, Hales P, Brindley DN. Unsaturated fatty acids activate glycogen phosphorylase in cultured rat hepatocytes. Biochem J 1991;276 (Pt 1):209–15
35. Gambert S, Héliès-Toussaint C, Grynberg A. Extracellular glycerol regulates the cardiac energy balance in a working rat heart model. Am J Physiol Heart Circ Physiol 2007;292:H1600–6
36. Copps KD, White MF. Regulation of insulin sensitivity by serine/threonine phosphorylation of insulin receptor substrate proteins IRS1 and IRS2. Diabetologia 2012;55:2565–82
37. Gual P, Le Marchand-Brustel Y, Tanti JF. Positive and negative regulation of insulin signaling through IRS-1 phosphorylation. Biochimie 2005;87:99–109
38. Li Y, Soos TJ, Li X, Wu J, Degennaro M, Sun X, Littman DR, Birnbaum MJ, Polakiewicz RD. Protein kinase C Theta inhibits insulin signaling by phosphorylating IRS1 at Ser(1101). J Biol Chem 2004;279:45304–7
39. Yu C, Chen Y, Cline GW, Zhang D, Zong H, Wang Y, Bergeron R, Kim JK, Cushman SW, Cooney GJ, Atcheson B, White MF, Kraegen EW, Shulman GI. Mechanism by which fatty acids inhibit insulin activation of insulin receptor substrate-1 (IRS-1)-associated phosphatidylinositol 3-kinase activity in muscle. J Biol Chem 2002;277:50230–6
40. Kim JK, Fillmore JJ, Sunshine MJ, Albrecht B, Higashimori T, Kim DW, Liu ZX, Soos TJ, Cline GW, O'Brien WR, Littman DR, Shulman GI. PKC-theta knockout mice are protected from fat-induced insulin resistance. J Clin Invest 2004;114:823–7
41. Bossenmaier B, Mosthaf L, Mischak H, Ullrich A, Häring HU. Protein kinase C isoforms beta 1 and beta 2 inhibit the tyrosine kinase activity of the insulin receptor. Diabetologia 1997;40:863–6
42. Strack V, Hennige AM, Krützfeldt J, Bossenmaier B, Klein HH, Kellerer M, Lammers R, Häring HU. Serine residues 994 and 1023/25 are important for insulin receptor kinase inhibition by protein kinase C isoforms beta2 and theta. Diabetologia 2000;43:443–9
43. Whittington RA, Virág L, Marcouiller F, Papon MA, El Khoury NB, Julien C, Morin F, Emala CW, Planel E. Propofol directly increases tau phosphorylation. PLoS One 2011;6:e16648
44. Hançer NJ, Qiu W, Cherella C, Li Y, Copps KD, White MF. Insulin and metabolic stress stimulate multisite serine/threonine phosphorylation of insulin receptor substrate 1 and inhibit tyrosine phosphorylation. J Biol Chem 2014;289:12467–84
45. Ni YG, Wang N, Cao DJ, Sachan N, Morris DJ, Gerard RD, Kuro-O M, Rothermel BA, Hill JA. FoxO transcription factors activate Akt and attenuate insulin signaling in heart by inhibiting protein phosphatases. Proc Natl Acad Sci U S A 2007;104:20517–22
46. Kovacic S, Soltys CL, Barr AJ, Shiojima I, Walsh K, Dyck JR. Akt activity negatively regulates phosphorylation of AMP-activated protein kinase in the heart. J Biol Chem 2003;278:39422–7
47. Horman S, Vertommen D, Heath R, Neumann D, Mouton V, Woods A, Schlattner U, Wallimann T, Carling D, Hue L, Rider MH. Insulin antagonizes ischemia-induced Thr172 phosphorylation of AMP-activated protein kinase alpha-subunits in heart via hierarchical phosphorylation of Ser485/491. J Biol Chem 2006;281:5335–40
48. Kewalramani G, An D, Kim MS, Ghosh S, Qi D, Abrahani A, Pulinilkunnil T, Sharma V, Wambolt RB, Allard MF, Innis SM, Rodrigues B. AMPK control of myocardial fatty acid metabolism fluctuates with the intensity of insulin-deficient diabetes. J Mol Cell Cardiol 2007;42:333–42
49. Tzatsos A, Tsichlis PN. Energy depletion inhibits phosphatidylinositol 3-kinase/Akt signaling and induces apoptosis via AMP-activated protein kinase-dependent phosphorylation of IRS-1 at Ser-794. J Biol Chem 2007;282:18069–82
50. Hunter RW, Treebak JT, Wojtaszewski JF, Sakamoto K. Molecular mechanism by which AMP-activated protein kinase activation promotes glycogen accumulation in muscle. Diabetes 2011;60:766–74
51. Andreozzi F, D'Alessandris C, Federici M, Laratta E, Del Guerra S, Del Prato S, Marchetti P, Lauro R, Perticone F, Sesti G. Activation of the hexosamine pathway leads to phosphorylation of insulin receptor substrate-1 on Ser307 and Ser612 and impairs the phosphatidylinositol 3-kinase/Akt/mammalian target of rapamycin insulin biosynthetic pathway in RIN pancreatic beta-cells. Endocrinology 2004;145:2845–57
52. Qi Y, Xu Z, Zhu Q, Thomas C, Kumar R, Feng H, Dostal DE, White MF, Baker KM, Guo S. Myocardial loss of IRS1 and IRS2 causes heart failure and is controlled by p38α MAPK during insulin resistance. Diabetes 2013;62:3887–900
53. Tremblay F, Brûlé S, Hee Um S, Li Y, Masuda K, Roden M, Sun XJ, Krebs M, Polakiewicz RD, Thomas G, Marette A. Identification of IRS-1 Ser-1101 as a target of S6K1 in nutrient- and obesity-induced insulin resistance. Proc Natl Acad Sci U S A 2007;104:14056–61

54. Meikle PJ, Wong G, Barlow CK, Weir JM, Greeve MA, MacIntosh GL, Almasy L, Comuzzie AG, Mahaney MC, Kowalczyk A, Haviv I, Grantham N, Magliano DJ, Jowett JB, Zimmet P, Curran JE, Blangero J, Shaw J. Plasma lipid profiling shows similar associations with prediabetes and type 2 diabetes. PLoS One 2013;8:e74341
55. Han MS, Lim YM, Quan W, Kim JR, Chung KW, Kang M, Kim S, Park SY, Han JS, Park SY, Cheon HG, Dal Rhee S, Park TS, Lee MS. Lysophosphatidylcholine as an effector of fatty acid-induced insulin resistance. J Lipid Res 2011;52:1234–46
56. Simões C, Silva AC, Domingues P, Laranjeira P, Paiva A, Domingues MR. Modified phosphatidylethanolamines induce different levels of cytokine expression in monocytes and dendritic cells. Chem Phys Lipids 2013;175-176:57–64
57. Leto D, Saltiel AR. Regulation of glucose transport by insulin: traffic control of GLUT4. Nat Rev Mol Cell Biol 2012;13:383–96
58. Watson RT, Pessin JE. Bridging the GAP between insulin signaling and GLUT4 translocation. Trends Biochem Sci 2006;31:215–22
59. Hotamisligil GS, Peraldi P, Budavari A, Ellis R, White MF, Spiegelman BM. IRS-1-mediated inhibition of insulin receptor tyrosine kinase activity in TNF-alpha- and obesity-induced insulin resistance. Science 1996;271:665–8
60. Heyland DK, MacDonald S, Keefe L, Drover JW. Total parenteral nutrition in the critically ill patient: a meta-analysis. JAMA 1998;280:2013–9